JOURNAL OF GEOPHYSICAL RESEARCH, VOL. 103, NO. B1, PAGES 691–705, JANUARY 10, 1998

# The shallow ice approximation for anisotropic ice: Formulation and limits

Anne Mangeney[1]

Laboratoire de Glaciologie et Geophysique de l'Environnement, CNRS, Saint Martin d'Heres, France

Francesco Califano

Scuola Normale Superiore, Pisa, Italy

**Abstract.** Ice sheet flow modeling is generally based on the shallow ice approximation (SIA) developed for isotropic ice. We extend this approximation to anisotropic ice and check its validity for both the isotropic and anisotropic cases by comparing the results of up to second-order SIA with those obtained from a model solving the full set of mechanical equations. The theory is developed for a constitutive relation describing Newtonian and non-Newtonian behavior, but numerical results are shown only for a Newtonian behavior. The results are compared for plane flow of isothermal ice under steady state conditions. SIA gives an excellent representation of the Newtonian flow of an isotropic ice sheet and a good description for the anisotropic case. The zero-order approximation is sufficient to describe ice flow precisely over flat bedrock, for the anisotropic and isotropic cases, even close to an ice divide. For uneven bedrock, the second-order SIA gives excellent results for isotropic ice and acceptable results for anisotropic ice. Finally, we quantify the error introduced by using an enhancement factor to represent the anisotropy when longitudinal stresses are taken into account.

## 1. Introduction

Solving the complete set of mechanical equations that describe the flow of an ice sheet requires long and difficult numerical calculations. For this reason, an approximate solution (the shallow ice approximation, hereinafter SIA) has been formulated. The aim of this paper is to systematically investigate the validity of this approximation which has often been done arbitrarily in the past, and to formulate the SIA taking into account the anisotropic behavior of ice.

The simplest model used to describe ice sheet flow considers the ice sheet as a parallel slab of infinite horizontal length, sliding over bedrock of uniform slope [*Nye*, 1952, 1957]. More complex approximate solutions have been formulated, including one based on an appropriate scale analysis of the field equations and boundary conditions (the SIA) [*Hutter*, 1981; *Fowler and Larson*, 1980]. This approximation gives explicit expressions for the velocity and stress field of a glacier when the bedrock topography and surface elevation slowly vary with respect to the horizontal coordinate $x$.

[1]Now at Institut de Physique du Globe de Paris, Paris, France.



Paper number 97JB02539.
0148-0227/98/97JB-02539$09.00

The SIA for isotropic ice was developed by *Hutter* [1981] and *Fowler and Larson* [1980]. The zero order of this approximation is now commonly used in ice sheet modeling [*Hutter*, 1993]. In the last few years, attempts have been made to solve the higher orders of this approximation numerically accounting for longitudinal stresses [*Dahl-Jensen*, 1989a, b; *Herterich*, 1988; *Blatter*, 1995], but as pointed out by *Hutter* [1993], no rigorous solution is yet available in the literature.

Mechanical tests in laboratories and deformation measurements in ice sheets have shown that the mechanical response of polar ice strongly depends on the direction of the prescribed stress. It is known that this viscoplastic anisotropy is linked to a preferred orientation of the crystallographic network of the grains contained in the sample (texture). The evidence of this strong anisotropy requires the use of an anisotropic constitutive relation to describe ice sheet flow. A realistic constitutive relation should be able to describe both the viscoplastic response of the material for a given texture and the evolution of the texture during the deformation. But no analytical constitutive relation taking both phenomena into account is available at present. Therefore we use here *Lliboutry*'s [1993] analytical constitutive relation that gives the anisotropic response of the material when the texture exhibits a revolution axis.

This paper addresses (1) the problem of a rigorous development of the zero, first and second order of SIA

in the case of isotropic and anisotropic ice, (2) the comparison of the results of the zero- and second-order approximation in both the isotropic and anisotropic cases with those obtained using a numerical model (the "complete" model) solving the complete set of mechanical equations [*Mangeney et al.*, 1996, 1997].

In section 2, after a brief description of the problem, we develop the zero, first and second order of the SIA and we describe the numerical model used to solve the SIA equations up to the second order. These theoretical results were obtained for a constitutive relation including a Newtonian ($n = 1$) and a non-Newtonian ($n = 3$) term. Here the numerical results are shown only for the Newtonian case. In section 3 we study the validity and limits of the SIA for the Newtonian case by comparing the solution with an "exact" numerical calculation. Furthermore, for flat and irregular bedrock, we discuss the relative magnitude of the different terms of the second-order approximation and we demonstrate that all the terms have to be taken into account for a correct calculation. Finally, in section 5 we quantify the extent of the error introduced by the use of an enhancement factor to describe the anisotropic viscoplastic behavior of ice [*Shoji and Langway*, 1984; *Dahl-Jensen*, 1985; *Kostecka and Whillans*, 1988; *Reeh and Paterson*, 1988; *Dahl-Jensen*, 1989a; *Schott et al.*, 1992].

## 2. Description of the Problem

### 2.1. Field Equations and Boundary Conditions

We consider the case of a steady state plane flow in two-dimensional slab geometry with a free surface $z = E(x)$ and a prescribed temperature field within the ice sheet over undulating bedrock $z = B(x)$ (Figure 1). We obtain dimensionless equations by using the ice depth $d_*$ as a characteristic depth and the typical accumulation rate at the upper free surface $u_*$ as a characteristic ice velocity (in this work we take $u_* = 0.2$ m.y.$^{-1}$ and $d_* = 2500$ m). A characteristic stress is defined by $\tau_* = \varrho g d_*$, where $\varrho$ is the ice density and $g$ the acceleration due to gravity; $\tau_*$ corresponds to the hydrostatic pressure at the base of the glacier. The dimensional variables are indicated by a tilde. Dimensionless variables are then given by

$$(x, z, E, B, H) = (\tilde{x}, \tilde{z}, \tilde{E}, \tilde{B}, \tilde{H})/d_*, \tag{1a}$$

$$(u, w) = (\tilde{u}, \tilde{w})/u_*, \tag{1b}$$

$$(S', p) = (\tilde{S}', \tilde{p})/\tau_*, \tag{1c}$$

$$D_{ij} = \tilde{D}_{ij} d_*/u_*, \tag{1d}$$

$$M_{ijkl} = \tilde{M}_{ijkl} u_*/(\tau_* d_*). \tag{1e}$$

Here $H$ is the ice thickness, $u$ and $w$ are the horizontal and vertical component of the velocity field $\mathbf{u}$, $D_{ij}$ and $S'_{ij}$ are the components of the strain rate tensor $\mathbf{D}$ and the deviatoric stress tensor $\mathbf{S}'$, respectively. The fluid pressure is indicated by $p$ and the viscosity tensor by $\mathbf{M}$. Let us call in this paper $(1a)_1$,$(1a)_2$, the first and second column of (1a), respectively.

The plane $(x - z)$ is assumed to be a symmetry plane for the flow of the ice sheet (i.e., $\partial/\partial y = 0$):

$$\frac{\partial p}{\partial y} = \frac{\partial S'_{yy}}{\partial y} = D_{yy} = S'_{yz} = S'_{xy} = 0. \tag{2}$$

The equations of mass and momentum conservation, in dimensionless form, read

$$\frac{\partial u}{\partial x} + \frac{\partial w}{\partial z} = 0, \tag{3}$$

$$\frac{\partial S'_{xx}}{\partial x} + \frac{\partial S'_{xz}}{\partial z} - \frac{\partial p}{\partial x} = 0,$$

$$\frac{\partial S'_{xz}}{\partial x} + \frac{\partial S'_{zz}}{\partial z} - \frac{\partial p}{\partial z} = 1. \tag{4}$$

We shall assume that the fluid is at rest at the undeformable base and that the top surface is stress free. Defining $\mathbf{n}_s$ as the unit normal vector at the surface, the boundary conditions read

$$\text{at } z = B(x): \quad \mathbf{u} = 0, \tag{5}$$

$$\text{at } z = E(x): \quad \sigma \cdot \mathbf{n}_s - p_{\text{atm}} \mathbf{n}_s = 0, \tag{6}$$

where $p_{\text{atm}}$ is the atmospheric pressure. At the upper surface $z = E(x)$, the kinematic surface equation reads

$$\frac{\partial E}{\partial t} + u \frac{\partial E}{\partial x} - w = a, \tag{7}$$

where $a$ is the accumulation rate. More details about these boundary conditions are given by *Mangeney* [1996] and *Mangeney et al.* [1996].

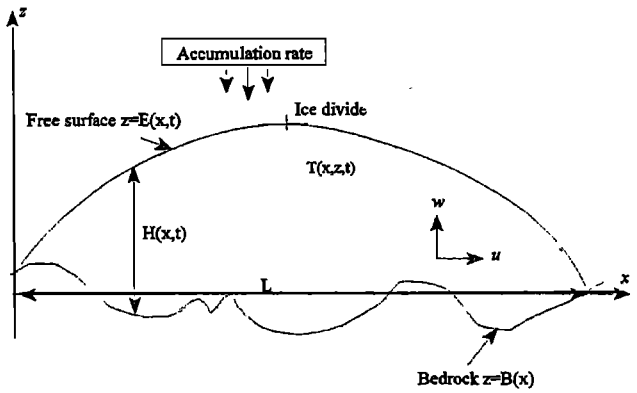


**Figure 1.** Cross section of a typical polar ice sheet.

### 2.2. Constitutive Relation

In ice sheet flow modeling, Glen's flow law is generally used to describe isotropic ice behavior [*Glen*, 1955; *Nye*, 1957 ]:

$$D_{ij} = A_n \tau^{n-1} S'_{ij}, \tag{8}$$

where $A_n$ is the temperature-dependent rate factor:

$$A_n = A_n^0 \exp(-Q/RT), \tag{9}$$

and $\tau$ the effective stress defined as

$$\tau^2 = \frac{1}{2} tr(\mathbf{S}'^2) \tag{10}$$

where $n$ is the stress sensitivity, $Q$ the activation energy for creep, $R$ the gas constant, and $T$ the absolute temperature.

Uncertainties exist concerning the value of the stress sensitivity $n$ in the constitutive relation. While 3 is the value for equivalent deviatoric stresses larger than about 0.2 MPa, both mechanical tests and borehole tilt measurements lead to a value lower than 2 [*Pimienta and Duval*, 1987; *Alley*, 1992] for lower stresses. *Doake and Wolff* [1985] have concluded from the data analysis of four boreholes that a linear approximation of the constitutive relation may be as appropriate as the commonly used nonlinear constitutive relation. For this reason we use here the constitutive relation with a Newtonian ($n = 1$) and a non-Newtonian ($n = 3$) term. In the isotropic case the constitutive relation reads

$$D_{ij} = \left(A_3 \tau^2 + A_1\right) S'_{ij}. \tag{11}$$

To describe the viscoplastic anisotropic response of the ice for a given texture, we use here the constitutive relation proposed by *Lliboutry* [1993] for orthotropic, transversally isotropic polar ice and applied to a plane flow by *Mangeney et al.* [1996]. This constitutive relation is based on a homogenization theory, assuming a uniform stress state within the polycrystal.

The texture is assumed to be a function of the reduced depth only and it does not depend on the deformation history of the ice. Texture development with reduced depth $\overline{z} = (z - B)/H$ was fitted on the fabric data of the recent Greenland Ice Core Project ice core [*Thorsteinsson et al.*, 1997] that represents a typical texture distribution for ice sheets (Figure 2a). The texture is randomly oriented at the surface and the ice is then isotropic. Deeper down, the ice crystals strongly concentrate around the vertical in situ direction (single maximum texture). As a consequence, the ice easily deforms when subjected to horizontal shear but strongly resists all longitudinal stresses. For a plane flow and with the particular texture symmetries we consider, the viscosity matrix has the form:

$$\begin{bmatrix} S'_{xx} \\ S'_{yy} \\ S'_{zz} \\ S'_{xz} \end{bmatrix} = \begin{bmatrix} M_1 & M_6 & M_5 & 0 \\ M_6 & M_2 & M_4 & 0 \\ M_5 & M_4 & M_3 & 0 \\ 0 & 0 & 0 & M_7 \end{bmatrix} \begin{bmatrix} D_{xx} \\ D_{yy} \\ D_{zz} \\ D_{xz} \end{bmatrix}, \tag{12}$$

where $M_1 = M_{xxxx}$, $M_2 = M_{yyyy}$, $M_3 = M_{zzzz}$, $M_4 =$

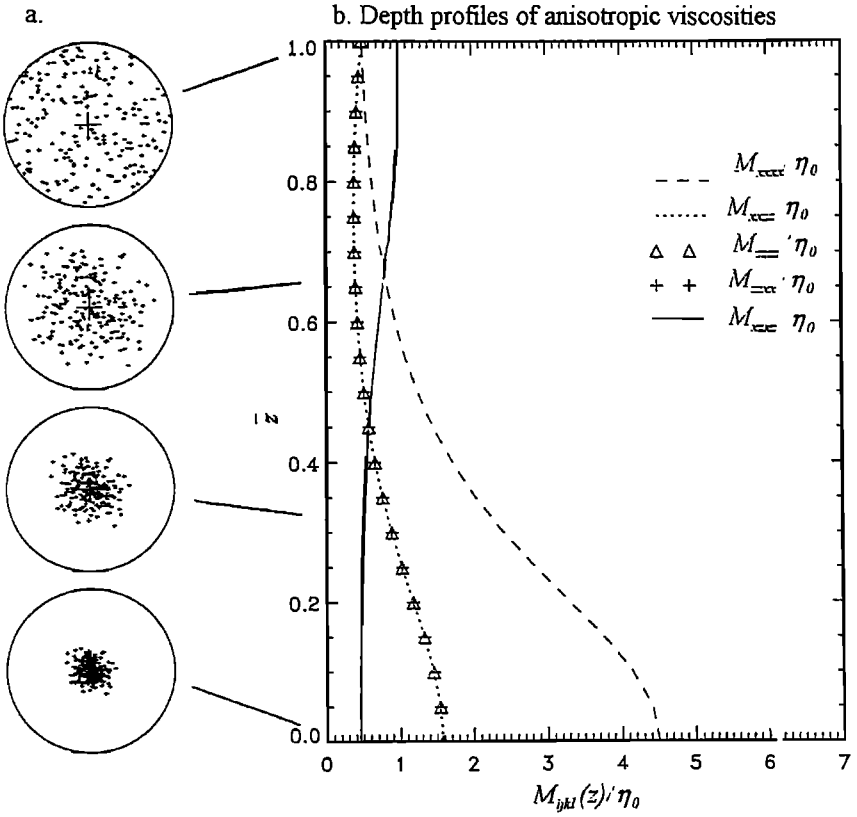


**Figure 2.** Characteristics of the fabric used in the model and the associated directional viscosities. (a) Development of the texture at 0, 1/4, 1/2, 3/4 and 1 times the depth. (b) Components of the viscosity matrix resulting from this texture. The viscosity tensor components are various symbols.

$M_{yyzz} = M_{zzyy}$, $M_5 = M_{xxzz} = M_{zzxx}$, $M_6 = M_{xxyy} = M_{yyxx}$ and $M_7 = M_{xzxz}$.

The dependence of the viscosity matrix components $M_{ijkl}$ on the four invariants of the deviatoric stress tensor is given by *Lliboutry* [1993] and *Mangeney et al.* [1996]. At the surface (isotropic ice), this constitutive relation is reduced to the generalized Glen's flow law (11) and the viscosity matrix reads

$$M_{ijkl} = \frac{1}{A_3\tau^2 + A_1} I_{ijkl}, \tag{13}$$

where $\mathbf{I}$ is the identity tensor. The variation of $M_{ijkl}$ with reduced depth in the Newtonian case is shown in Figure 2. In this work, we impose an ice temperature of $-20^0$C and the value of $A_1 = 2.8 \times 10^3$ [*Duval and Castelnau*, 1995] and $A_3 = 2.6 \times 10^8$ [*Budd and Jacka*, 1989] ($\tilde{A}_1 = u_*/(\tau_* d_*)A_1$ and $\tilde{A}_3 = u_*/(\tau_*^3 d_*)A_3$). In the numerical results presented here only $A_1$ is used (Newtonian behavior).

### 2.3. Shallow Ice Approximation

We will now briefly recall the main features of the SIA [*Hutter*, 1983, pp. 270-331; *Morland*, 1984]. This approximation is based on the slow variation of the ice sheet geometry and bedrock topography with respect to the horizontal coordinate $x$. This approximation has been widely used in the other branches of fluid mechanics, for example, to solve the shallow water equations in the theory of surface gravity waves [see, e.g., *Friedrichs*, 1948; *Keller*, 1948]. We introduce coordinate stretching such that the surface variation in the horizontal direction ($\partial E/\partial X$) and the velocity components in the new coordinates are $\mathcal{O}(1)$:

$$X = \epsilon x, \quad Z = z, \tag{14}$$

$$U = \epsilon u_x, \quad W = u_z. \tag{15}$$

The aspect ratio $\epsilon$ is a small parameter defined by the ratio between the characteristic ice thickness $d_*$ and the characteristic length of the glacier $L_*$:

$$\epsilon = d_*/L_*. \tag{16}$$

Typical values are $\epsilon = 10^{-3}$ for Antarctic and $5 \times 10^{-3}$ for Greenland [*Paterson*, 1994, p. 262]. All the fields $\psi$ are assumed to vary slowly with the horizontal coordinate $x$ ($\psi = \psi(\epsilon x, z)$). Using the stretched coordinates, (3) and (4) become

$$\frac{\partial U}{\partial X} + \frac{\partial W}{\partial Z} = 0, \tag{17}$$

$$\epsilon\left(-\frac{\partial p'}{\partial X} + \frac{\partial S'_{xx}}{\partial X}\right) + \frac{\partial S'_{xz}}{\partial Z} = 0, \tag{18a}$$

$$\epsilon\frac{\partial S'_{xz}}{\partial X} - \frac{\partial p'}{\partial Z} + \frac{\partial S'_{zz}}{\partial Z} - 1 = 0, \tag{18b}$$

with the boundary conditions (6) at the upper surface now transformed to

$$S'_{xz}(1 - \epsilon^2\Gamma^2) = \epsilon\Gamma(S'_{xx} - S'_{zz}) \quad z = E(x)$$

$$(1 - \epsilon^2\Gamma^2)p' = S'_{zz} - \epsilon^2\Gamma^2 S'_{xx} \quad z = E(x), \tag{19}$$

where

$$\frac{\partial E}{\partial x} = \epsilon\frac{\partial E}{\partial X} = \epsilon\Gamma, \quad p' = p - p_{\mathrm{atm}}.$$

All terms in (17), (18) and (19) must be expressed in terms of powers of $\epsilon$ with coefficients of order unity to get $f(\epsilon, \epsilon^2, \text{etc.}) = 0$. Only then can the coefficients of each power of $\epsilon$ be set to be identically zero. The deviatoric stress $\mathbf{S}'$ has not yet been expanded in powers of $\epsilon$; such an expansion is now necessary. For this reason we express the constitutive relation in terms of the velocity gradients in the new coordinates:

$$S'_{xx} = M_{xxxx}\frac{\partial U}{\partial X} + M_{xxzz}\frac{\partial W}{\partial Z}, \tag{20a}$$

$$S'_{zz} = M_{zzxx}\frac{\partial U}{\partial X} + M_{zzzz}\frac{\partial W}{\partial Z}, \tag{20b}$$

$$S'_{xz} = M_{xzxz}\frac{1}{2}\left(\frac{1}{\epsilon}\frac{\partial U}{\partial Z} + \epsilon\frac{\partial W}{\partial X}\right). \tag{20c}$$

We assume here that all the components $M_{ijkl}$ of the viscosity matrix are of the same order. Indeed, the viscosities are all equal at the surface, because the ice is isotropic there and are of the same order in the upper half of the ice sheet. Therefore no other small parameter linked with the anisotropy can be introduced even though the viscosity in response to shear stresses may be at least 1 order of magnitude lower than the viscosity in response to longitudinal stresses, close to the bedrock. Then, from (20), $S'_{xx} \sim \epsilon S'_{xz}$ and in equation (18) the leading order terms are the horizontal pressure gradient and the vertical gradient of the shear stress. The stresses were dimensionalized by $\tau_*$ so that $p'$ is $\mathcal{O}(1)$. This requires that $S'_{xz}$ is $\mathcal{O}(\epsilon)$. We introduce new components $\mathcal{M}_{ijkl}$ in the viscosity matrix which are $\mathcal{O}(1)$. This implies from (20c) and from the order of magnitude of the shear stress that

$$\mathcal{M}_{ijkl} = \frac{M_{ijkl}}{\epsilon^2}. \tag{21}$$

This variable change corresponds to that obtained by *Hutter* [1983, p. 313] for the isotropic case, who found that, in the case of a power law with exponent $n$, $\mathcal{A}_{ijkl}$ in the new coordinates of order 1 satisfies $A_n = \mathcal{A}_n/\epsilon^{n+1}$. Indeed, the effective stress $\tau$ being $\mathcal{O}(\epsilon)$, (13) reads

$$M_{ijkl} = \epsilon^2\frac{1}{\mathcal{A}_3\mathcal{T}^2 + \mathcal{A}_1} I_{ijkl}, \tag{22}$$

where $\mathcal{T} = \tau/\epsilon$ is $\mathcal{O}(1)$. We then obtain the deviatoric stress components, a function of the viscosity matrix components in the new coordinates:

$$S'_{xx} = \epsilon^2 \left( \mathcal{M}_{xxxx} \frac{\partial U}{\partial X} + \mathcal{M}_{xxzz} \frac{\partial W}{\partial Z} \right),$$

$$S'_{zz} = \epsilon^2 \left( \mathcal{M}_{zzxx} \frac{\partial U}{\partial X} + \mathcal{M}_{zzzz} \frac{\partial W}{\partial Z} \right),$$

$$S'_{xz} = \epsilon \mathcal{M}_{xzxz} \frac{1}{2} \left( \frac{\partial U}{\partial Z} + \epsilon^2 \frac{\partial W}{\partial X} \right). \quad (23)$$

Another method would be to introduce the scale factor $\epsilon$ between the "shear" viscosity $M_{xzxz}$ and the "longitudinal" viscosities in order to take into account the fact that anisotropic ice strongly resists compression or traction but is weaker with respect to shear. With this scaling, we obtain the following relation:

$$M_{xzxz} = \epsilon^3 \mathcal{M}_{xzxz},$$

$$M_{iiii} = \epsilon^2 \mathcal{M}_{iiii}, \quad i,j = x,z$$

$$M_{iijj} = \epsilon^2 \mathcal{M}_{iijj}.$$

This scaling leads to the same zero-order SIA as the scaling used in (21). Another possible approach is a multiple scales analysis. In this case, in addition to the scale factor $\epsilon$ related to the ice sheet geometry, a small new parameter $\epsilon_a$ related to the ice anisotropy is introduced. This approach also gives the same zero-order results (A. Salamatin, personal communication, 1996).

Expressing all the quantities in terms of a power series of $\epsilon$ [*Hutter*, 1983, p. 274] in (17), (18) and (19) we solve the zero-, first- and second-order SIA. The details of the calculation are given in the appendix.

### 2.4. Numerical Models

The zero-order terms of the solution series for steady, isothermal and isotropic plane flow of a grounded ice sheet have been presented by *Morland and Johnson* [1980, 1982]. The steady state approximation was solved numerically by *Yakowitz et al.* [1986] and *Hutter et al.* [1986, 1987], and the nonsteady state has been calculated by many glaciologists in order to quantify the behavior of large ice sheets under various climatic variations [*Hindmarsh et al.*, 1987, 1989; *Herterich*, 1988; *Hindmarsh and Hutter*, 1988; *Calov*, 1990; *Huybrechts*, 1990a, b; *Huybrechts and Oerlemans*, 1990; *Letreguilly et al.*, 1991a, b; *Fabre et al.*, 1995]. At zero order, the effects of longitudinal strain rates are not taken into account. In the model of *Hutter et al.* [1986], based on the zero-order solution, a significant quantity of basal sliding is required to obtain accurate predictions. This model is limited due to the fact that longitudinal strain rates are neglected despite their importance in the vicinity of an ice divide [*Szidarovsky et al.*, 1989]. The solution of the first-order equations is identically equal to zero for the velocity field (see Appendix), so that it is necessary to solve the second-order system to take these effects into account. We present here the solution of the SIA in the general case of an anisotropic constitutive relation up to second order. This solution has never been formulated nor used, to the authors' knowledge.

To solve the equations of the SIA up to the second order, we numerically integrate the set of equations (A4)-(A9) coupled with (A17) which represent the free-surface changes. For the zero-order system, the fields depend only on $E^{(0)}$ and on its derivatives. It is therefore possible to calculate first the zero-order approximation of the flow and free-surface changes, then the second-order approximation.

The calculation is obtained by successive iterations of the flow and free-surface equations until a steady state is reached. In particular, the time dependent free-surface equations are solved using a semi-implicit version of the standard second-order (explicit) Adams-Bashford scheme [*Peyret and Taylor*, 1983; *Mangeney*, 1996].

The evaluation of the validity of the SIA is made using a "complete" model solving the set of mechanical equations in a fixed domain including the ice divide (this solution will hereinafter be referred to as the "exact" solution). The numerical code used to solve the complete mechanical equations is discussed by *Mangeney* [1996] and by *Mangeney et al.* [1997]. The margin position is not calculated.

Horizontal velocity profiles are imposed at the left and right boundaries of the domain. In the shallow ice model we impose the surface elevation at both right and left boundaries so that the ice divide elevation calculated with the SIA model is the same as the ice divide elevation previously calculated with the "complete" model.

## 3. Results

In this work we use a linear viscosity to compare different order solutions of the SIA for isothermal flow for the isotropic and anisotropic case with the "exact" solution.

### 3.1. Flat Bedrock

In this section we will start from the simplest situation, that of flat bedrock. In Figure 3 we plot the surface elevation (Figures 3a and 3b) and the vertical velocity at the surface (Figures 3c and 3d) versus $x$, for the zero-order (Figures 3a and 3c) and second-order (Figures 3b and 3d) terms. The solution represents an equilibrium configuration for each the isotropic and anisotropic case with an accumulation rate $a(x) = 1$.

From this figure, it is immediately evident that the zero-order approximation gives a very good representation of the ice flow on flat bedrock for the isotropic as well as the anisotropic case. More specifically, Figures 3b-3d show that the second-order correction is practically negligible everywhere.

The same behavior is also observed in the other physical fields, such as the horizontal velocity and the shear

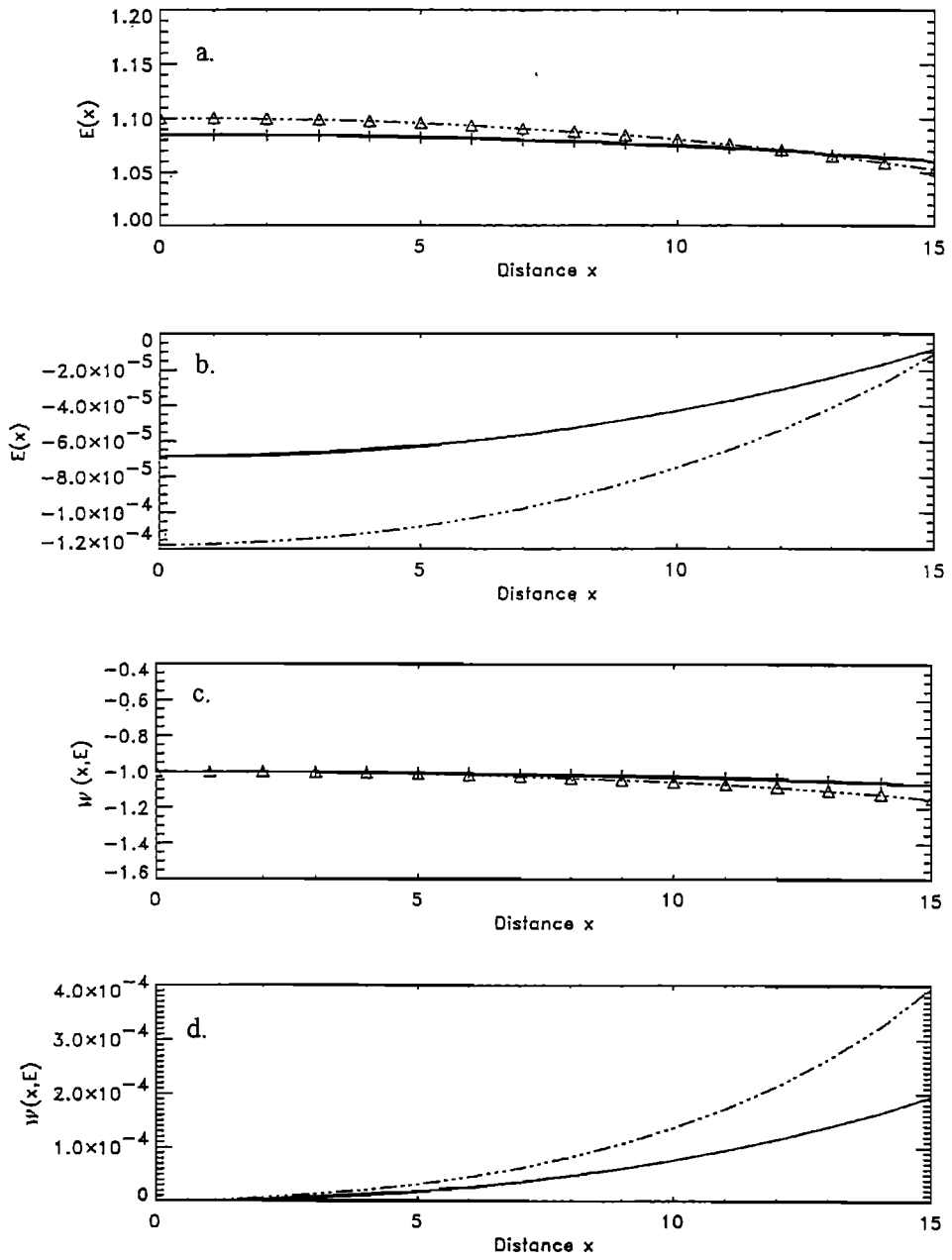


**Figure 3.** (a) Surface elevation and (c) vertical velocity at the surface calculated with the complete model. Dashed-dotted lines refer to the isotropic case and solid lines refer to the anisotropic case. Triangles and plus signs refer to the zero-order SIA for the isotropic and anisotropic case, respectively. (b, d) Second-order terms of the SIA for the surface elevation and the vertical velocity, respectively, for the isotropic (dashed-dotted lines) and anisotropic (solid lines) cases.

stress, except for the longitudinal stresses which, as expected from the analytical development, have a vanishing zero-order approximation. Furthermore, we observe in Figure 4 that the first-order approximation of the longitudinal stresses in the anisotropic case is in very good agreement with the results of the "exact" solution. We have obtained the same result for the isotropic case.

### 3.2. Irregular Bedrock

Ice sheet flow over uneven bedrock is a current problem. Indeed, 30 km from the future European Programme for Ice Coring in Antarctica drill site at Dome C (Antarctica), the bedrock topography varies over 10 km from -600 to +800 m compared to the sea surface elevation; this corresponds to a variation of 50% of the ice thickness over less than four ice thicknesses. In order to study the validity of the SIA in the presence of irregular bedrock, we define a sinusoidal bedrock

$$B = B_0 \cos\left(2\pi f \frac{x}{L}\right), \tag{24}$$

in the domain $|x| < L/2$, where $L = 30$ in dimension-

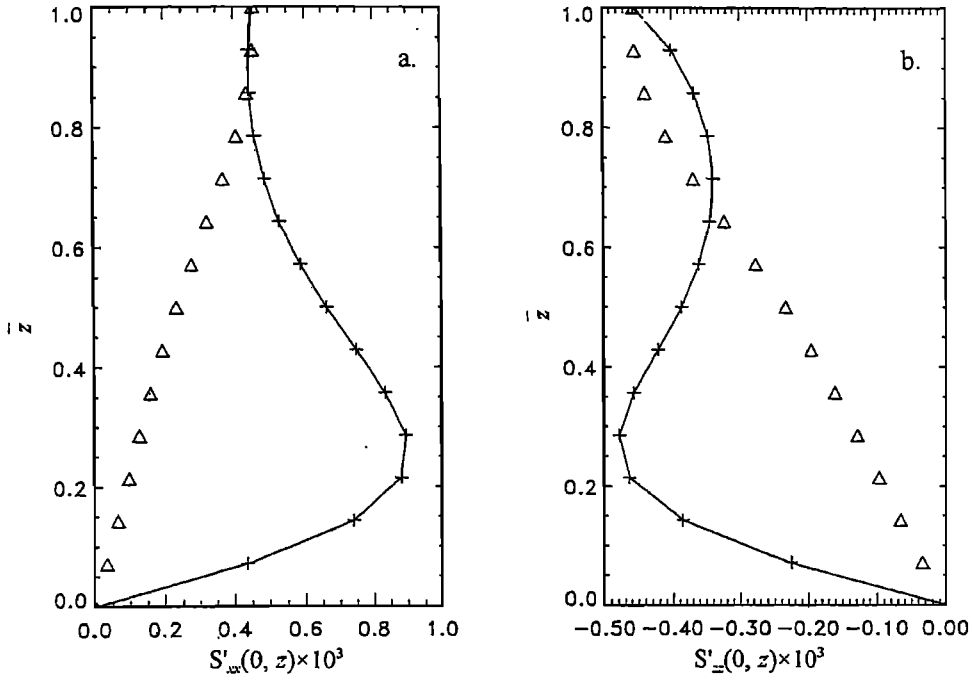


**Figure 4.** Vertical profiles of (a) the longitudinal stress and (b) the axial stress at the ice divide in the anisotropic case, obtained with the complete model (solid lines), the second-order SIA (plus signs) and the second-order SIA with the anisotropic viscosity tensor replaced by an isotropic flow law with a depth-dependent enhancement factor (triangles). The stresses are multiplied by a factor of $10^3$.

less variables. For $|x| > 15$ the bedrock elevation $B$ is taken to be equal to $-B_0$. Here $f$ and $B_0$ are the frequency and the amplitude of the undulations, respectively. Note that for $|x| < 10$, the solution is independent of the bedrock topography imposed for $|x| > 15$. In what follows we have taken a fixed value of the frequency $f = 3$ and of the amplitude $B_0 = 0.2$. However, a number of calculations with different values of $f$ and $B_0$ (not discussed here) have been performed. These calculations show that results are not qualitatively affected by the choice of $f$ and $B_0$. We emphasize that the numerical values of $f$ and $B_0$ are such that the maximum gradient of the bedrock $\partial B/\partial x$ is $\mathcal{O}(\epsilon)$; therefore the SIA is still valid. We have also checked that for the anisotropic case the horizontal viscosity gradients $\partial M_{ijkl}/\partial x$ are also $\mathcal{O}(\epsilon)$. As for the flat bedrock, the solution represents an equilibrium configuration for each the isotropic and anisotropic case with an accumulation rate $a(x) = 1$. A detailed description of the comparison between the isotropic and anisotropic case is given by *Mangeney et al.* [1996, 1997]. We show here only results providing a clear comparison between the SIA and the "exact" solution.

In Figure 5 we show the shear stress at three different locations, $x = 1$ near the ice divide, $x = 5$ within a "bedrock hole" and $x = 10$ over a "bedrock bump." The isotropic case is shown in the first three illustrations, and the anisotropic case is shown in the last three illustrations. In the isotropic case we see that the zero-order approximation gives a relatively good representation of the "exact" solution; very good agreement is reached with the second-order correction. In the anisotropic case, on the other hand, we observe that the zero-order approximation is a rough estimate of the "exact" solution. In fact, in Figures 5d-5f we see that it is necessary to include the second-order terms in the calculation to obtain a reasonable estimate of the real flow. However, there are some locations, for example, at $x = 5$, where even the second-order approximation strays far from the "exact" solution. This effect is particularly evident on the profile of the longitudinal stress (Figure 6).

The observed disagreement of the SIA with respect to the "exact" solution for the anisotropic case can be explained by the appearance of strong gradients of longitudinal stresses $\partial S'_{xx}/\partial x$. In fact, in this case these gradients can achieve typical values roughly equal to or greater than the surface slope corresponding to the horizontal gradient of the pressure in the zero-order system (see equation (A4)), so that they cannot be neglected at the zero order (equation (18)). These high values of the gradient are observed mainly in the basal layers over the holes. It can be explained by the fact that the longitudinal stresses themselves are very high in the basal layers, which act as a stress guide because of their stiffness to extension. The overlaying layers are able to deform enough to satisfy strain rate continuity with the deep stiff layers without the need for high stress. The upper layers, if stressed longitudinally, respond quickly by flow in order to relax or lower the stress, because they, being isotropic, are not hard to extend. The deep layers,

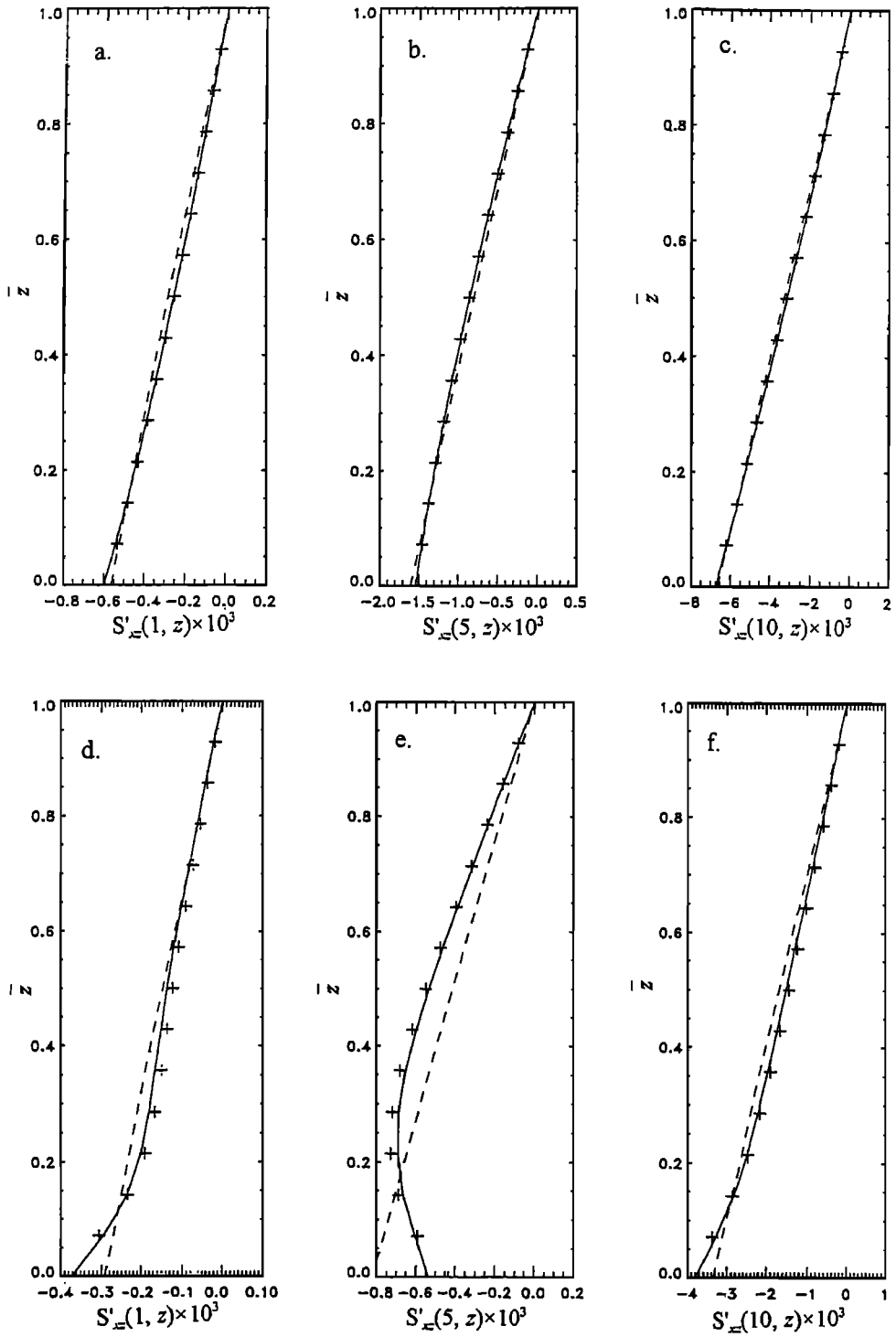


**Figure 5.** Vertical profiles of the shear stress for uneven bedrock for the isotropic case (a) at $x = 1$ (near the ice divide), (b) at $x = 5$ (over a hole), (c) at $x = 10$ (over a bump) and for the anisotropic case (d) at $x = 1$, (e) at $x = 5$ and (f) at $x = 10$; results obtained with the complete model are shown by solid lines, those obtained with the zero-order SIA by dashed lines and those calculated with the second-order SIA by plus signs. The stresses are multiplied by a factor of $10^3$.

on the other hand, being more viscous for longitudinal extension, cannot respond as quickly and so remain perpetually supporting more than their "fair share" of the driving longitudinal stress (Ed. Waddington, personal communication, 1997).

One of the most interesting results is that the SIA is very satisfactory in the vicinity of the ice divide, where this approximation was thought to fail until present. In fact, the scale analysis used for the SIA does not require the horizontal velocity $u$ to be different from

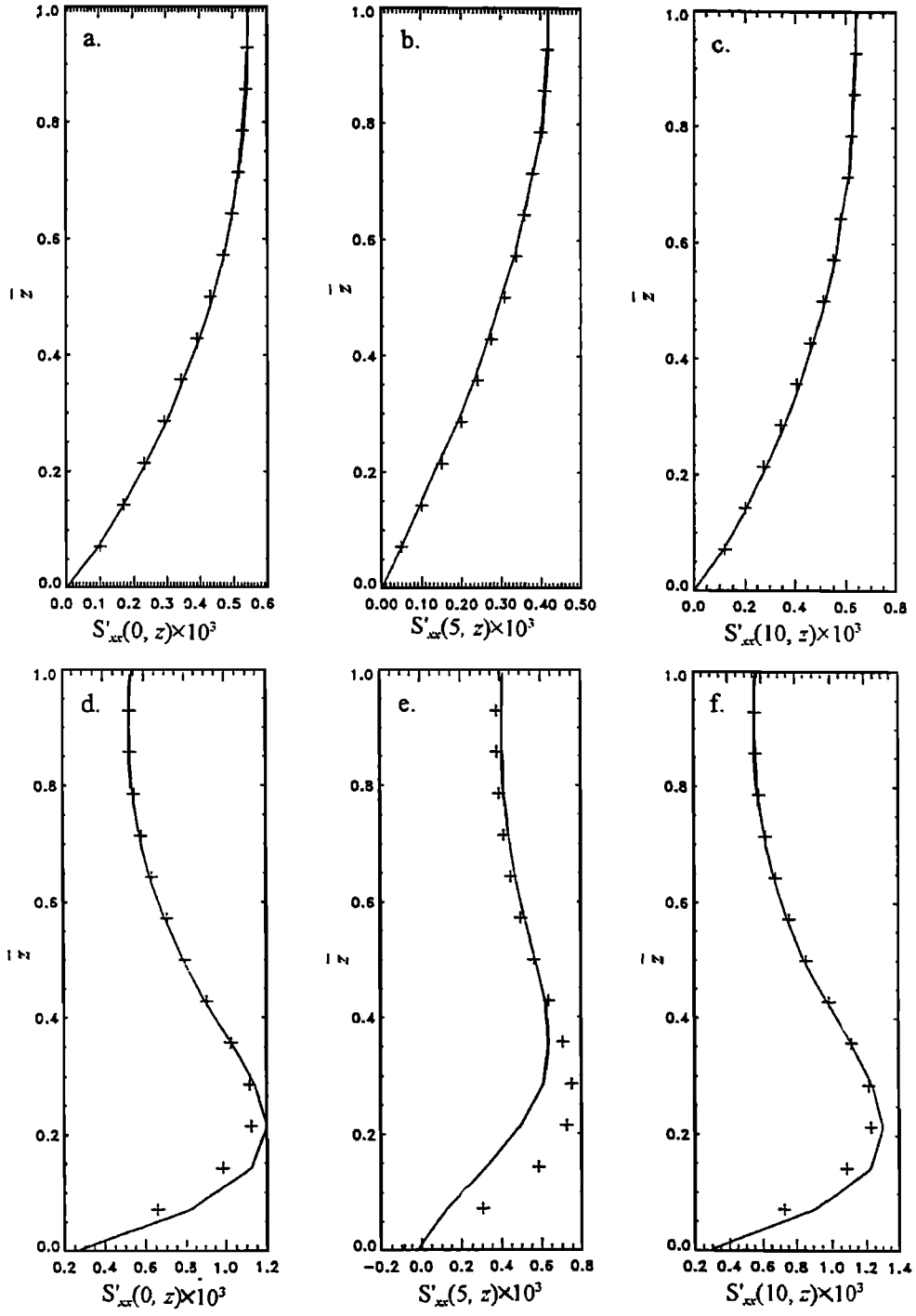


**Figure 6.** Vertical profiles of the longitudinal stress for uneven bedrock for the isotropic case (a) at $x = 0$ (at the ice divide), (b) at $x = 5$ (over a hole), (c) at $x = 10$ (over a bump) and for the anisotropic case (d) at $x = 0$, (e) at $x = 5$ and (f) at $x = 10$; results obtained with the complete model are shown by solid lines and those calculated with the second-order SIA by plus signs. The stresses are multiplied by a factor of $10^3$.

zero everywhere (see equation (15)); on the other hand, if the absolute value of $\partial u/\partial x$ is $\mathcal{O}(\epsilon)$ or less where $u = 0$, then the assumptions of the SIA are no longer satisfied [*Mangeney*, 1996].

### 3.3. Magnitudes of Second-Order Terms

At the second order the shear stress (A14) is given by

$$S'^{(2)}_{xz} = -\frac{\partial}{\partial X}\int_E^Z \left(S'^{(1)}_{xx} - S'^{(1)}_{zz}\right) dz' + \int_E^Z \int_E^Z \frac{\partial^2 S'^{(0)}_{xz}}{\partial X^2} dz' dz'' + \left(\Gamma^{(0)^3} + \Gamma^{(2)}\right)\left(z - E^{(0)}\right) - \Gamma^{(0)} E^{(2)} \quad (25)$$

Note that $S'^{(2)}_{xz}$ takes into account the effects of longitudinal strain rates. According to *Hutter* [1981], the magnitude of this second-order correction term significantly depends on the exponent of the constitutive relation and, as we will show later, it also depends on the viscoplastic anisotropy of the ice.

The zero-order solution is not valid in regions where the longitudinal strain rates are significant. For this reason many authors have tried to incorporate the longitudinal strain rates in ice sheet flow modeling. *Szidarovsky et al.* [1989] have numerically evaluated the second-order SIA, but their numerical procedure, starting from the ice divide, is based on an ad hoc vertical velocity profile imposed at the ice divide. Another approach was to use the zero-order approximation to calculate the vertical stress:

$$\sigma_{xx} = \sigma_{zz} = -p' = E - Z, \tag{26}$$

and then to calculate the shear stress using the equations of the second-order SIA [*Dahl-Jensen*, 1989a, b; *Herterich*, 1988; *Blatter*, 1995]. The expression of the shear stress deduced by this method is

$$S'_{xz} = \frac{\partial E}{\partial x}(z - E) - 2\int_E^z \frac{\partial S'_{xx}}{\partial x} dz' \tag{27}$$

and, comparing with the second-order correction of the shear stress (25), we see that some terms have been arbitrarily neglected. We observe, as was pointed out by *Hutter* [1993], that this method is not rigorous because the zero- and second-order SIA are mixed arbitrarily; the zero-order equation (26) implies that the normal stresses are not material dependent [*Hutter*, 1993]. Despite the efforts to evaluate the magnitude of different terms contained in the second-order shear stress [*Budd*, 1971; *Hutter et al.*, 1981; *Kamb and Echelmeyer*, 1986a, b, c, d], a correct calculation of the relative magnitude of these terms has never been made even for the isotropic case. The exact evaluation of these terms is of significant importance when flow models are used as an inverse method to determine rheological parameters, for example.

To obtain an estimate of the relative magnitude of the different terms of the second-order shear stress, we express $S'^{(2)}_{xz}$ as a sum of four terms: $S'^{(2)}_{xz} = A + B + C + D$ with

$$\begin{aligned} A &= -\frac{\partial}{\partial X}\int_E^Z \left(S'^{(1)}_{xx} - S'^{(1)}_{zz}\right) dz', \\ B &= \int_E^Z \int_E^Z \frac{\partial^2 S'^{(0)}_{xz}}{\partial X^2} dz' dz'', \\ C &= \Gamma^{(0)^3}\left(z - E^{(0)}\right), \\ D &= \Gamma^{(2)}\left(z - E^{(0)}\right) - \Gamma^{(0)}E^{(2)}. \end{aligned} \tag{28}$$

In Figure 7 we show the second-order basal shear stress versus $x$ for both the isotropic and anisotropic case together with the individual components $A$, $B$, $C$ and $D$. In the isotropic case (Figure 7a), we observe that all the different terms are of the same order of magnitude,

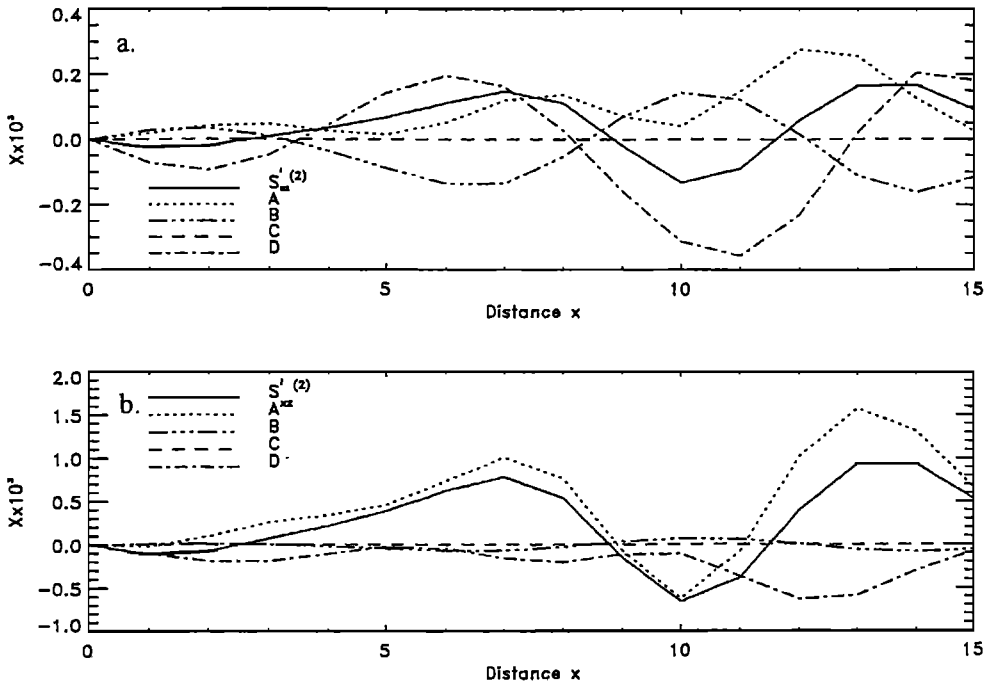


**Figure 7.** Second-order terms of the SIA for the basal shear stress versus the ice divide distance (a) for the isotropic and (b) anisotropic case. The different terms $X = (A, B, C, D)$ involved in the basal shear stress at second order are also plotted. The stresses are multiplied by a factor of $10^3$.

except $C$, which turns out to be negligible with respect to the others. In the anisotropic case (Figure 7b) we see that term $A$ is predominant, even if $D$ should be taken into account.

As discussed above, the only term included in the previous "second-order numerical models" is the first term $A$, the others being arbitrarily neglected. Therefore the results obtained in this way are necessarily inconsistent. This inconsistency is particularly flagrant given that all these models are limited to the isotropic case. It is worth noting that in most cases these models have been applied to flows on almost flat bedrock. This explains the rather good agreement with "exact" solutions such as the one calculated by *Schott Hvidberg* [1996]. In fact, as discussed above, the second order correction is in such cases negligible with respect to the zero order solution (except for the longitudinal stresses); therefore the terms $B$, $C$ and $D$ are effectively negligible, as well as the term $A$. However, with flat bedrock, this approach is equivalent to solving the SIA up to the second order.

## 4. On the Use of an Enhancement Factor

In order to take anisotropy into account, many authors assume that the parameter $A_n^0$ in the constitutive relation (8) is a function of the structure of polar ice. This factor $A_n^0$ has been assumed to be dependent mainly on texture [*Hooke*, 1981; *Budd and Jacka*, 1989]. This dependence is commonly taken into account by assuming that $A_n^0$ is proportional to a depth-dependent enhancement factor $\mathcal{E}(z)$ [*Shoji and Langway*, 1984; *Dahl-Jensen*, 1985; *Kostecka and Whillans*, 1988; *Reeh and Paterson*, 1988; *Dahl-Jensen*, 1989a; *Schott et al.*, 1992; C. Schott Hvidberg et al., Ice flow between the GRIP and GISP2 boreholes in central Greenland, submitted to *Journal of Geophysical Research*, 1996]. Note that in this case the constitutive relation is still isotropic. This method is, of course, not correct when longitudinal stresses are taken into account. The use of the enhancement factor $\mathcal{E}(z)$ to represent the anisotropy is equivalent to replacing the isotropic viscosity $\eta_0$ by the shear viscosity $M_{xzxz}$ ($\mathcal{E}(z) = M_{xzxz}/\eta_0$). We will here quantify the extent of the error introduced by the scalar enhancement factor.

Equation (29) shows that the zero-order horizontal velocity is inversely proportional to the component $M_{xzxz}$ of the viscosity tensor (equation (A12) of the appendix):

$$U^{(0)}(X,Z) = U^{(0)}(X,B) - \int_B^Z \frac{2\Gamma^{(0)}}{M_{xzxz}}(E^{(0)} - zl)dzl. \tag{29}$$

In what follows, we call $M_{xxxx}$, $M_{xxzz}$, $M_{zzxx}$, and $M_{zzzz}$ the axial viscosities, and we call $M_{xzxz}$ the shear viscosity. Since the shear stress is the only component of the deviatoric stress unequal to zero, the zero-order approximation for the anisotropic case is equivalent to the use of an enhancement factor $\mathcal{E}(z) = M_{xzxz}/\eta_0$ in the isotropic viscosity. The method of using an enhancement factor to calculate the flow of anisotropic ice is then correct for the zero-order approximation.

However, when the second-order correction is calculated, that is, when the longitudinal stresses are taken into account, this enhancement factor does not correspond to an exact representation of the anisotropy. The second term of the second-order shear stress, equation (25), is compatible with this enhancement factor because the shear stresses are the same in the isotropic and anisotropic case, while the first term will introduce significant error. In ice with $c$ axes aligned with the vertical axis, and the ice is more resistant to longitudinal stress and less resistant with respect to shear stress. However, the enhancement factor introduced in the isotropic viscosity leads to the same value for axial and shear viscosities. From Figure 2 it is clear that the four axial viscosities have a completely different shape than that of $M_{xzxz}$ and vary in the opposite sense: the shear viscosity component decreases with depth, while the others increase. Therefore the enhancement factor used to represent the axial viscosities makes the ice less resistant to longitudinal stresses, exactly the contrary of the real effect. Even if this contradiction occurs essentially in the deep layers where longitudinal stresses are small, we will show below that this has an influence on the flow. As pointed out by *Van der Veen and Whillans* [1990], anisotropy must be taken into account at least by different rate factors for different strain rate components. From Figure 4, we see that the longitudinal and axial stresses obtained using the enhancement factor are completely different from the "exact" solution.

In Figures 8a-8d we plot the shear and longitudinal stress and the horizontal and vertical velocity at $x = 5$, respectively. In this figure we observe that the "consistent" second-order SIA in the anisotropic case gives a rather good representation of the flow obtained by the complete calculation. On the other hand, the second-order correction obtained using an enhancement factor is practically negligible with respect to the zero-order solution, which means that it is not the correct way to approach the "exact" solution starting from the zero-order approximation. As expected theoretically, the longitudinal stress calculated using the enhancement factor is wrong. These results are independent of the particular point $x = 5$ considered in Figure 8.

## 5. Conclusion

In this paper we address the problem of the shallow ice approximation (SIA) developed by *Hutter* [1983, pp. 270-331] for the isotropic case and extended here to the anisotropic case. The main goal was to check the validity of this approximation. This was achieved by comparing the results of the SIA up to the second order to

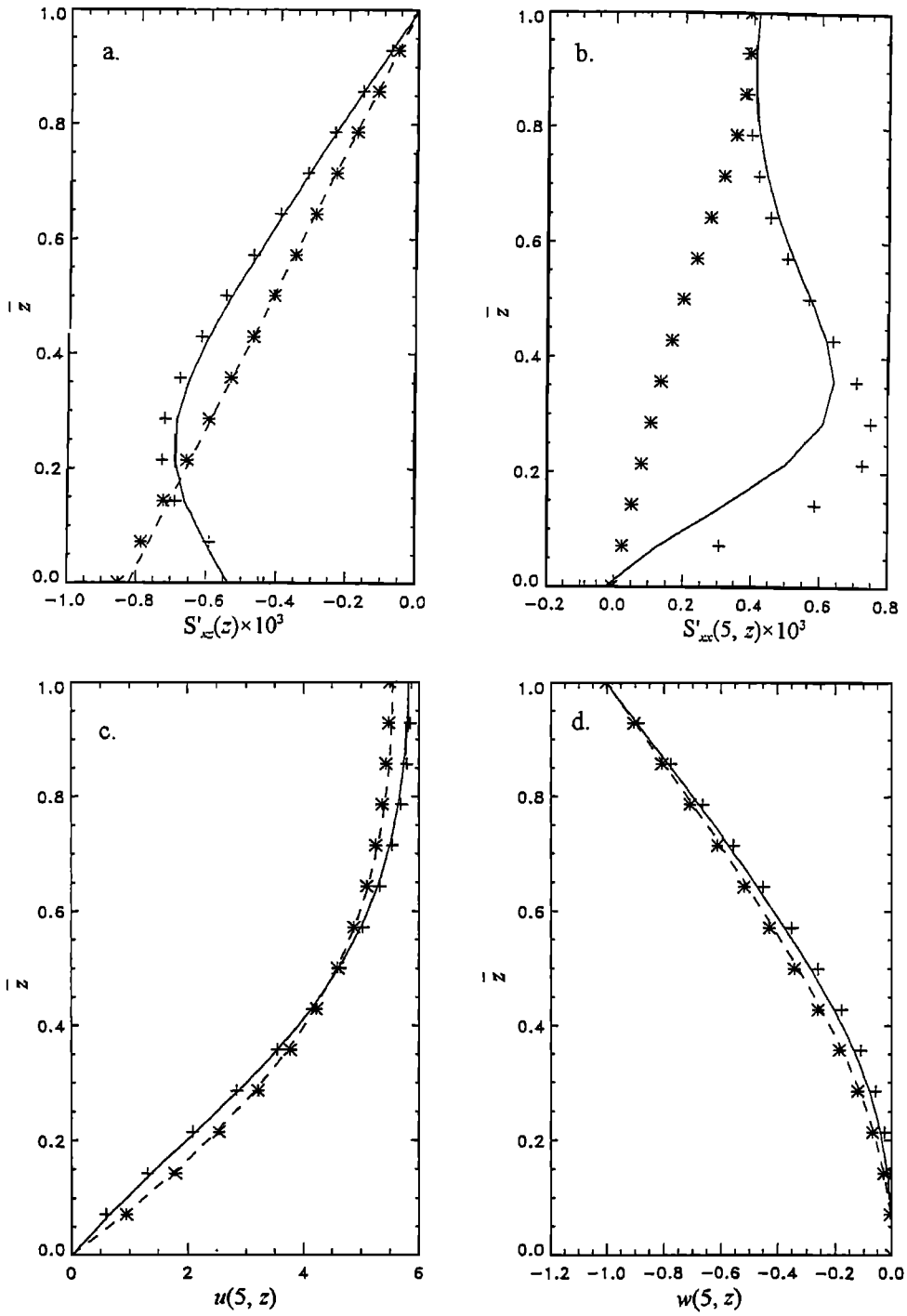


**Figure 8.** Vertical profiles at $x = 5$ of the (a) shear stress, (b) the longitudinal stress, (c) the horizontal velocity and (d) the vertical velocity for the anisotropic case; the results obtained using the complete model are shown by solid lines, those corresponding to the zero-order approximation by dashed lines, those obtained with the second-order SIA by plus signs and those calculated with an enhancement factor by asterisks. The longitudinal stresses of the zero-order approximation are equal to zero. The stresses are multiplied by a factor of $10^3$.

an "exact" numerical solution obtained by integrating the full set of mechanical equations.

The most important result is that the SIA gives an excellent representation of the Newtonian flow of an isotropic ice sheet and a good description for the anisotropic case. When flat bedrock is considered, the zero-order approximation of the SIA is sufficient to describe "exactly" the flow for isotropic, as well as anisotropic case. We stress that, as opposed to what was thought before, the SIA remains valid even in the vicinity of an ice divide for a Newtonian behavior.

When significant perturbations are introduced on the bedrock profile, up to 50% of the ice depth over a typical length of five ice thicknesses, the zero-order SIA

still gives a good approximation of the flow for isotropic case. A further expansion to the second order then gives excellent agreement with the "exact" solution.

On the other hand, for the anisotropic case, the zero-order solution is a very rough approximation of the "exact" solution, so that it is necessary to improve the calculation by including second-order terms. In this case, the maximum relative error on the stresses is of order of 10%. This result comes from the fact that strong horizontal gradients of the longitudinal stress are generated close to the holes of the bedrock. The presence of these strong gradients modifies the mechanical balance in the zero-order system between the vertical gradient of the shear stress and the surface slope. Finally, we have quantified the error introduced by using an enhancement factor in the isotropic viscosity to model anisotropic effects.

Since this work was a first step in validating the SIA and to improve it by incorporating an anisotropic constitutive relation, we have limited our analysis to isothermal situations. This condition can be easily removed in order to obtain more realistic results. The SIA and the "exact" solution were compared for a given ice divide elevation calculated in a fixed domain. Since the SIA is not applicable close to the margins, the surface elevation obtained with this approximation can be different from that obtained with a complete model in which the movement of the boundaries is taken into account.

## Appendix: Solution of the Shallow Ice Approximation up to Second Order in the General Case of Anisotropic Ice

We give here the detailed solution of (17) and (18) with boundary conditions (19) using the perturbation method in a power series of the aspect ratio $\epsilon$. Expressing all the quantities as a power series of $\epsilon$ [*Hutter*, 1983, pp. 274],

$$(p', U, W, E) = \sum_j \epsilon^j (P^{(j)}, U^{(j)}, W^{(j)}, E^{(j)}), \quad \text{(A1)}$$

in (23) at the third order we have

$$\begin{aligned}
S'_{xx} &= \epsilon^2 \mathcal{M}_{xxxx}\left(\frac{\partial U^{(0)}}{\partial X} + \epsilon\frac{\partial U^{(1)}}{\partial X}\right) \\
&\quad + \epsilon^2 \mathcal{M}_{xxzz}\left(\frac{\partial W^{(0)}}{\partial Z} + \epsilon\frac{\partial W^{(1)}}{\partial Z}\right), \\
S'_{zz} &= \epsilon^2 \mathcal{M}_{zzxx}\left(\frac{\partial U^{(0)}}{\partial X} + \epsilon\frac{\partial U^{(1)}}{\partial X}\right) \\
&\quad + \epsilon^2 \mathcal{M}_{zzzz}\left(\frac{\partial W^{(0)}}{\partial Z} + \epsilon\frac{\partial W^{(1)}}{\partial Z}\right), \\
S'_{xz} &= \epsilon \mathcal{M}_{xzxz}\frac{1}{2}\left(\frac{\partial U^{(0)}}{\partial Z} + \epsilon\frac{\partial U^{(1)}}{\partial Z} + \epsilon^2\frac{\partial U^{(2)}}{\partial Z}\right) \\
&\quad + \epsilon \mathcal{M}_{xzxz}\frac{1}{2}\left(\epsilon^2\frac{\partial W^{(0)}}{\partial X}\right). \quad \text{(A2)}
\end{aligned}$$

Since the deviatoric stresses are of an order less than or equal to $\epsilon$, we develop the stresses as

$$\begin{aligned}
S'_{xz} &= \epsilon\left(S'^{(0)}_{xz} + \epsilon S'^{(1)}_{xz} + \epsilon^2 S'^{(2)}_{xz}\right) \\
S'_{xx} &= \epsilon\left(S'^{(0)}_{xx} + \epsilon S'^{(1)}_{xx} + \epsilon^2 S'^{(2)}_{xx}\right) \\
S'_{zz} &= \epsilon\left(S'^{(0)}_{zz} + \epsilon S'^{(1)}_{zz} + \epsilon^2 S'^{(2)}_{zz}\right). \quad \text{(A3)}
\end{aligned}$$

Introducing (A1), (A2) and (A3) in (17), (18) and (19), we obtain zero-, first- and second-order equations.

**Zero-order equations**

$$\frac{\partial U^{(0)}}{\partial X} + \frac{\partial W^{(0)}}{\partial Z} = 0, \quad S'^{(0)}_{xx} = 0, \quad \text{(A4a)}$$

$$-\frac{\partial P^{(0)}}{\partial X} + \frac{\partial S'^{(0)}_{xz}}{\partial Z} = 0, \quad S'^{(0)}_{zz} = 0, \quad \text{(A4b)}$$

$$\frac{\partial P^{(0)}}{\partial Z} = -1, \quad S'^{(0)}_{xz} = \mathcal{M}_{xzxz}\frac{1}{2}\frac{\partial U^{(0)}}{\partial Z}, \quad \text{(A4c)}$$

with boundary conditions at the surface

$$\mathcal{M}_{xzxz}\frac{1}{2}\frac{\partial U^{(0)}}{\partial Z} = 0, \quad \text{(A5a)}$$

$$P^{(0)} = 0. \quad \text{(A5b)}$$

**First-order equations**

$$\frac{\partial U^{(1)}}{\partial X} + \frac{\partial W^{(1)}}{\partial Z} = 0, \quad \text{(A6a)}$$

$$-\frac{\partial P^{(1)}}{\partial X} + \frac{\partial S'^{(1)}_{xz}}{\partial Z} = 0, \quad \text{(A6b)}$$

$$\frac{\partial P^{(1)}}{\partial Z} = 0, \quad \text{(A6c)}$$

$$S'^{(1)}_{xx} = \mathcal{M}_{xxxx}\frac{\partial U^{(0)}}{\partial X} + \mathcal{M}_{xxzz}\frac{\partial W^{(0)}}{\partial Z}, \quad \text{(A6d)}$$

$$S'^{(1)}_{zz} = \mathcal{M}_{zzxx}\frac{\partial U^{(0)}}{\partial X} + \mathcal{M}_{zzzz}\frac{\partial W^{(0)}}{\partial Z}, \quad \text{(A6e)}$$

$$S'^{(1)}_{xz} = \mathcal{M}_{xzxz}\frac{1}{2}\frac{\partial U^{(1)}}{\partial Z}, \quad \text{(A6f)}$$

with boundary conditions at the surface

$$\mathcal{M}_{xzxz}\frac{1}{2}\frac{\partial U^{(1)}}{\partial Z} = 0, \quad \text{(A7a)}$$

$$P^{(1)} = 0. \quad \text{(A7b)}$$

**Second-order equations**

$$\frac{\partial U^{(2)}}{\partial X} + \frac{\partial W^{(2)}}{\partial Z} = 0, \quad \text{(A8a)}$$

$$-\frac{\partial P^{(2)}}{\partial X} + \frac{\partial S'^{(1)}_{xx}}{\partial X} + \frac{\partial S'^{(2)}_{xz}}{\partial Z} = 0, \quad \text{(A8b)}$$

$$-\frac{\partial P^{(2)}}{\partial Z} + \frac{\partial S'^{(0)}_{xz}}{\partial X} + \frac{\partial S'^{(1)}_{zz}}{\partial Z} = 0, \quad \text{(A8c)}$$

$$S'^{(2)}_{xx} = \mathcal{M}_{xxxx}\frac{\partial U^{(1)}}{\partial X} + \mathcal{M}_{xxzz}\frac{\partial W^{(1)}}{\partial Z}, \quad \text{(A8d)}$$

$$S'^{(2)}_{zz} = \mathcal{M}_{zzxx}\frac{\partial U^{(1)}}{\partial X} + \mathcal{M}_{zzzz}\frac{\partial W^{(1)}}{\partial Z}, \quad \text{(A8e)}$$

$$S'^{(2)}_{xz} = \mathcal{M}_{xzxz}\frac{1}{2}\left(\frac{\partial U^{(2)}}{\partial Z} + \frac{\partial W^{(0)}}{\partial X}\right), \quad \text{(A8f)}$$

with boundary condition at the surface

$$S'^{(2)}_{xz} - \Gamma^{(0)}\left(S'^{(1)}_{xx} - S'^{(1)}_{zz}\right) + \frac{\partial S'^{(0)}_{xz}}{\partial Z}E^{(2)} = 0,$$

$$P^{(2)} + \frac{\partial P^{(0)}}{\partial Z}E^{(2)} = S'^{(1)}_{zz}, \quad \text{(A9)}$$

where

$$\Gamma^0 = \frac{\partial E^{(0)}}{\partial X}.$$

### A1. Zero-Order Solution

Integration of equation $(A4c)_1$ with the boundary condition (A5b) gives

$$P^{(0)} = E^{(0)} - Z. \quad \text{(A10)}$$

Integration of $(A4b)_1$ with the boundary condition (A5a) gives the shear stress

$$S'^{(0)}_{xz} = -\Gamma^{(0)}(E^{(0)} - Z). \quad \text{(A11)}$$

Note that (A4) leads to $S'^{(0)}_{xx} = S'^{(0)}_{zz} = 0$. Integrating $(A4c)_2$ with respect to $z$ using slip conditions at the bedrock gives

$$U^{(0)}(X,Z) = U^{(0)}(X,B) - \int_B^Z \frac{2\Gamma^{(0)}}{\mathcal{M}_{xzxz}}(E^{(0)} - z')dz'. \quad \text{(A12)}$$

The continuity equation $(A4a)_1$ allows us to calculate $W$ by integrating with respect to $z$ from the bedrock

$$W^{(0)}(X,Z) = W^{(0)}(X,B) - \int_B^Z \frac{\partial U^{(0)}}{\partial X}dz'. \quad \text{(A13)}$$

### A2. First-Order Solution

The solution of the first-order equations (A6) and (A7) is identically equal to zero, except for the longitudinal stresses given by (A6d) et (A6e).

### A3. Second-Order Solution

We differentiate (A8b) with respect to $z$ and substract the $x$ derivative of (A8c). Then, using boundary conditions (A9) and the Leibnitz rule, we integrate twice with respect to $z$, obtaining the expression for the shear stress:

$$\begin{aligned} S'^{(2)}_{xz} &= -\frac{\partial}{\partial X}\int_E^Z \left(S'^{(1)}_{xx} - S'^{(1)}_{zz}\right)dz' \\ &+ \int_E^Z\int_E^Z \frac{\partial^2 S'^{(0)}_{xz}}{\partial X^2}dz'dz'' \\ &+ \left(\Gamma^{(0)^3} + \Gamma^{(2)}\right)\left(Z - E^{(0)}\right) \\ &- \Gamma^{(0)}E^{(2)}. \end{aligned} \quad \text{(A14)}$$

Taking into account (A8f), $U^{(2)}$ is calculated as function of the zero-order solution only:

$$\begin{aligned} U^{(2)}(X,Z) &= U^{(2)}(X,B) - \int_B^Z \frac{\partial W^{(0)}}{\partial X}dz' \\ &+ \int_B^Z \frac{2S'^{(2)}_{xz}}{\mathcal{M}_{xzxz}}dz', \end{aligned} \quad \text{(A15)}$$

and $W^{(2)}$ is calculated integrating (A8a):

$$W^{(2)}(X,Z) = W^{(2)}(X,B) - \int_B^Z \frac{\partial U^{(2)}}{\partial X}dz'. \quad \text{(A16)}$$

### A4. Surface Elevation

The first order being identically equal to zero, $E = E^{(0)} + \epsilon^2 E^{(2)}$, equation (7) reads

$$\frac{\partial E^{(0)}}{\partial t} + U^{(0)}\frac{\partial E^{(0)}}{\partial X} - W^{(0)} = a,$$

$$\frac{\partial E^{(2)}}{\partial t} + U^{(0)}\frac{\partial E^{(2)}}{\partial X} + U^{(2)}\frac{\partial E^{(0)}}{\partial X} - W^{(2)} = 0. \quad \text{(A17)}$$

**Acknowledgments.** We thank the Observatoire de Paris-Meudon (DESPA) for the use of their facilities. This work was supported by the Programme National d'Etude du Climat (PNEDC), the environment program of the CCE (in France), and the EISMINT program (European Science Foundation). We are grateful to K. Hutter and Y. Ricard for fruitful discussions. We thank Waddington for deep review of this paper.

## References

Alley, R. B., Flow-law hypotheses for ice sheet modeling, *J. Glaciol.*, *38*(129), 245-256, 1992.

Blatter, H., Velocity and stress fields in grounded glaciers: A simple algorithm for including deviatoric stress gradients, *J. Glaciol.*, *41*(138), 333-343, 1995.

Budd, W. F., Stress variations with ice flow over undulations, *J. Glaciol.*, *10*(59), 177-195, 1971.

Budd, W. F., and T. H. Jacka, A review of ice rheology for ice sheet modelling, *Cold Reg. Sci. Technol.*, *16*, 107-144, 1989.

Calov, R., *Modellierung des Gronandischen Inlandeises mit Einem Dreidimensionalen Inlandeismodell*, Dtsch. Forsch., Bonn, Germany, 1990.

Dahl-Jensen, D., Determination of the flow properties at Dye 3, south Greenland, by bore-hole-tilting measurements and perturbation modelling, *J. Glaciol.*, *31*(108), 92-98, 1985.

Dahl-Jensen, D., Two dimensional thermomechanical modelling of flow and depth-age profiles near the ice divide in central Greenland, *Ann. Glaciol.*, *12*, 31-36, 1989a.

Dahl-Jensen, D., Steady thermomechanical flow along two-dimensional flow lines in large grounded ice sheets, *J. Geophys. Res.*, *94*, 10,355-10,362, 1989b.

Doake, C. S. M., and E. W. Wolff, Flow law for ice in polar ice sheets, *Nature*, *314*(6008), 255-257, 1985.

Duval, P., and O. Castelnau, Dynamic recrystallization of ice in polar ice sheets, *J. Phys. IV*, *5*, 197-205, 1995.

Fabre, A., A. Letreguilly, C. Ritz, and A. Mangeney, Greenland under changing climates: Sensitivity experiments with a new three-dimensional ice-sheet model, *Ann. Glaciol.*, *21*, 1-7, 1995.

Fowler, A. C., and D. A. Larson, The uniqueness of steady state flows of glaciers and ice sheets, *Geophys. J. R. Astron. Soc.*, *63*, 333-345, 1980.

Friedrichs, K. O., Water waves on shallow sloping beach, *Commun. Pure Appl. Math.*, *1*, 109-134, 1948.

Glen, J. W., The creep of pollycrystalline ice, *Proc. R. Soc. London*, A, *228*(1175), 519-538, 1955.

Herterich, K., A three-dimensional model of the Antarctic ice sheet, *Ann. Glaciol.*, *11*, 32-35, 1988.

Hindmarsh, R. C. A., and K. Hutter, Numerical fixed domain solution of free-surface flows coupled with an evolving interior field, *Int. J. Numer. Anal. Methods Geomech.*, *12*, 437-459, 1988.

Hindmarsh, R. C. A., L. W. Morland, G. S. Boulton, and K. Hutter, The unsteady plane flow of ice-sheets, a parabolic problem with two moving boundaries, *Geophys. Astrophys. Fluid Dyn.*, *39*(3), 183-225, 1987.

Hindmarsh, R. C. A., L. W. Morland, G. S. Boulton, and K. Hutter, Modes of operation of thermo-mechanically coupled ice-sheets, *Ann. Glaciol.*, *12*, 57-69, 1989.

Hooke, R. L., Flow law for polycrystalline ice in glaciers: Comparison of theoretical predictions, laboratory data, and field measurements, *Rev. Geophys.*, *19*(4), 664-672, 1981.

Hutter, K., The effect of longitudinal strain on the shear stress of an ice sheet: In defense of using stretched coordinates, *J. Glaciol.*, *27*(95), 39-56, 1981.

Hutter, K., *Theoretical Glaciology: Material Science of Ice and the Mechanics of Glaciers and Ice Sheets*, D. Reidel, Norwell, Mass., 1983.

Hutter, K., Thermo-mechanically coupled ice-sheet response : Cold, polythermal, temperate, *J. Glaciol.*, *39*(131), 65-86, 1993.

Hutter, K., F. Legerer, and U. Spring, First-order stresses and deformations in glaciers and ice sheets, *J. Glaciol.*, *27*(96), 227-270, 1981.

Hutter, K., S. Yakowitz, and F. Szidarovszky, A numerical study of plane ice-sheet flow, *J. Glaciol.*, *92*(11), 139-160, 1986.

Hutter, K., S. Yakowitz, and F. Szidarovszky, Coupled thermomechanical response of an axisymmetric cold ice sheet, *Water Resour. Res.*, *23*(7), 1327-1339, 1987.

Huybrechts, P., A 3-D model for the Antarctic ice-sheet: A sensitivity study on the glacial-interglacial contrast, *Clim. Dyn.*, *5*(2), 79-92, 1990a.

Huybrechts, P., The Antarctic ice sheet during the last glacial-interglacial cycle: A three-dimensional experiment, *Ann. Glaciol.*, *14*, 115-119, 1990b.

Huybrechts, P., and J. Oerlemans, Response of the Antarctic ice sheet to future greenhouse warming, *Clim. Dyn.*, *5*(2), 93-102, 1990.

Kamb, B., and K. A. Echelmeyer, Stress-gradient coupling in glacier flow, I, Longitudinal averaging of the influence of ice thickness and surface slope, *J. Glaciol.*, *32*(111), 267-284, 1986a.

Kamb, B., and K. A. Echelmeyer, Stress-gradient coupling in glacier flow, II, Longitudinal averaging in the flow response to small perturbations in ice thickness and surface slope, *J. Glaciol.*, *32*(111), 285-298, 1986b.

Kamb, B., and K. A. Echelmeyer, Stress-gradient coupling in glacier flow, III, Exact longitudinal equilibrium equations, *J. Glaciol.*, *32*(112), 335-341, 1986c.

Kamb, B., and K. A. Echelmeyer,, Stress-gradient coupling in glacier flow, IV, Effect of the "T" term, equation, *J. Glaciol.*, *32*(112), 342-349, 1986d.

Keller, J. B., The solitary wave and periodic waves in shallow water, *Commun. Pure Appl. Math.*, *1*, 329-339, 1948.

Kostecka, J. M., and I. M. Whillans, Mass balance along two transects of wide side of the Greenland ice-sheet, *J. Glaciol.*, *34*(116), 31-39, 1988.

Letreguilly, A., P. Huybrechts, and N. Reeh, Steady-state characteristics of the Greenland ice sheet under different climates, *J. Glaciol.*, *37*(125), 149-157, 1991a.

Letreguilly, A., N. Reeh, and P. Huybrechts, The Greenland ice-sheet through the last glacial-interglacial cycle, *Palaeogeogr. Palaeoclimatol. Palaeoecol.*, *90*(4), 385-394, 1991b.

Lliboutry, L., Anisotropic, transversally isotropic nonlinear viscosity of rock ice and rheological parameters inferred from homogenization, *Int. J. Plast.*, *9*, 619-632, 1993.

Mangeney, A., Modelisation de l'ecoulement de la glace dans les calottes polaires: Prise en compte d'une loi de comportement anisotrope, thesis, Univ. Pierre et Marie Curie, Paris, 1996.

Mangeney, A., F. Califano, and O. Castelnau, Isothermal flow of an anisotropic ice sheet in the vicinity of an ice divide, *J. Geophys. Res.*, *101*, 28,189-28,204, 1996.

Mangeney, A., F. Califano, and K. Hutter, A numerical study of anisotropic, low-Reynolds number, free surface flow for ice sheet modeling, *J. Geophys. Res.*, *102*, 22,749-22,764, 1997.

Morland, L. W., Thermomechanical balances of ice sheet flows, *Geophys. Astrophys. Fluid Dyn.*, *29*, 237-266, 1984.

Morland, L. W., and I. R. Johnson, Steady motion of ice sheets, *J. Glaciol.*, *25*(92), 229-246, 1980.

Morland, L. W., and I. R. Johnson, Effect on bed inclination and topography on steady isothermal ice sheets, *J. Glaciol.*, *28*(98), 71-90, 1982.

Nye, J. F., The mechanics of glacier flow, *J. Glaciol.*, *2*(12), 82-93, 1952.

Nye, J. F., The distribution of stress and velocity in glaciers and ice-sheets, *Proc. R. Soc. London A*, *239*, 113-133, 1957.

Paterson, W. S. B., *The Physics of Glaciers*, Pergamon, Tarrytown, N. Y., 1994.

Peyret, R., and T. D. Taylor, *Computational Methods in Fluid Flows*, Springer-Verlag, New York, 1983.

Pimienta, P., and P. Duval, Rate controlling processes in the creep of polar ice, *J. Physique C1*, *48*, suppl. 3, 243-248, 1987.

Reeh, N., and W. S. B. Paterson, Application of a flow model to the ice-divide of Devon Island ice cap, Canada, *J. Glaciol.*, *34*(116), 55-63, 1988.

Schott, C., E. D. Waddington, and C. F. Raymond, Predicted time-scales for GISP2 and GRIP boreholes at Summit, Greenland, *J. Glaciol.*, *38*(128), 162-168, 1992.

Schott Hvidberg, C., Steady state thermo-mechanical modelling of ice flow near the center of large ice sheets with the finite element technique, *Ann. Glaciol.*, *23*, 116-124, 1996.

Shoji, H., and C. C. Langway, Flow behavior of basal ice as related to modelling considerations, *Ann. Glaciol.*, *5*, 141-148, 1984.

Szidarovsky, F., K. Hutter, and S. Yakowitz, Computational ice-divide analysis of a cold plane ice sheet under steady conditions, *Ann. Glaciol.*, *12*, 170-177, 1989.

Thorsteinsson, T., J. Kipfstuhl, and H. Miller, Textures and fabrics in the GRIP ice core, *J. Geophys. Res.*, in press, 1997.

Van der Veen, C. J., and I. M. Whillans, Flow laws for glacier ice: Comparison of numerical predictions and field measurements, *J. Glaciol.*, *36*(124), 324-339, 1990.

Yakowitz, S., K. Hutter, and F. Szidarovsky, Elements of a computational theory for glaciers, *J. Comput. Phys.*, *66*(1), 132-150, 1986.

F. Califano, Scuola Normale Superiore, Piazza dei Cavalieri 7, 56100, Pisa, Italy. (e-mail: califano@cibs.sns.it)

A. Mangeney, Observatoires volcanologiques, IPGP, 4, Place Jussieu, 75005 Paris, France. (e-mail: mangeney@ipgp.jussieu.fr)

(Received July 12, 1996; revised June 18, 1997; accepted September 8, 1997.)